Zuerst ersch. in : Cell Cycle ; 10 (2011), 20. - S. 3533 - 3544
DOI : 10.4161/cc.10.20.17817

Modulated microtubule dynamics enable Hklp2/Kif15 to assemble bipolar spindles

Stefan Florian and Thomas U. Mayer

Konstanz Research School Chemical Biology; University of Konstanz; Konstanz, Germany

Key words: mitosis, mitotic spindle, Eg5, cancer treatment, microtubule dynamics

Activity of the sliding motor Eg5 and coordinated microtubule dynamics are both essential for mitotic spindle pole separation. It is still a matter of controversy if changes in microtubule dynamics can compensate inhibition of Eg5 activity and re-enable bipolarization. Using a consistent live cell-imaging approach, we show that perturbation of microtubule dynamics can compensate inhibition of Eg5 through a spindle formation process reminiscent of meiosis: In Eg5-inhibited mammalian somatic cells, alteration of microtubule dynamics through depletion of TOGp or low doses of nocodazole induces the formation of multiple acentrosomal spindle poles which pass through an intermediate multipolar state followed by bipolarization. Pole separation depends on Hklp2/Kif15, an otherwise dispensable plus end-directed spindle motor and results in spindles with two centrosomal poles. Once bipolar, spindles do not rely on altered microtubule dynamics to maintain their bipolarity anymore and are functional in chromosome segregation. We conclude that altered microtubule dynamics enable Hklp2/Kif15 to replace Eg5 in pole separation through a mechanism involving the formation of acentrosomal poles. Our observations suggest that combination chemotherapy regimens involving microtubule-targeting drugs and Eg5 inhibitors might be less effective than expected.

Introduction

The mitotic spindle is a bipolar structure responsible for accurate chromosome segregation during cell division.[1,2] It consists of microtubules and microtubule-associated proteins which can act as molecular motors and modulators of microtubule dynamics.[3-8] In somatic cells, the two spindle poles are formed by centrosomes, which constitute the main microtubule nucleation centers, while oocytes assemble acentrosomal meiotic spindles through a chromosomal nucleation process leading to an "inside-out" spindle formation process.[9,10] Pole separation depends on both the motor activity of the plus end-directed kinesin Eg5[11-18] and on precise coordination of microtubule dynamics.[19-24] Consequently, perturbation of either of them can result in the formation of monopolar spindles.[25] Based on its tetrameric structure, Eg5 is assumed to mediate pole separation by cross-linking and sliding apart overlapping interpolar microtubules.[15,26,27] Notably, inhibition of Eg5 does not cause the collapse of preformed bipolar spindles, demonstrating that Eg5 is required for the establishment but not maintenance of spindle bipolarity.[28] Eg5 or its homologs are also not required for anaphase in yeast or humans,[28-30] during which other molecular components seem to generate the chromosome-segregating force.[31] In the absence of Eg5 activity, spindle bipolarity is maintained by the activity of the plus end-directed kinesin Hklp2/Kif15, which, intriguingly, cannot complement the function of Eg5 in assembling bipolar spindles.[23,32,33] In the Xenopus egg extract system, it has been shown that Eg5 activity is also required for microtubule flux, the net movement of tubulin dimers within microtubule protofilaments from the spindle equator towards poles.[34,35] During development of mouse embryos, flux becomes independent of Eg5 activity, which might explain why spindles in these embryos do not rely anymore on Eg5 activity to maintain spindle bipolarity.[36] Thus, there is ample evidence that molecular motors regulate microtubule dynamics. However, the degree of functional redundancy between the two systems is still a matter of controversy. In experiments based on immunofluorescence analyses of fixed samples,[21] it was found that low doses of the microtubule drug nocodazole were not able to restore bipolarity if Eg5 was inhibited. In contrast, Kollu et al. could rescue bipolar spindle formation in Eg5-inhibited cells when microtubules were destabilized by the depletion of astrin, and this effect was suppressed by the microtubule stabilizer taxol, whereas the depletion of the microtubule destabilizer MCAK rendered spindles dependent on Eg5 activity even when bipolarity was established. These observations led to the hypothesis that the extent of overlapping microtubules, i.e., the zone of force generation, which is large during spindle assembly and upon MCAK depletion and low in bipolar spindles and upon astrin depletion, determines if Eg5 activity is required for bipolarity. However, in general, it is still unclear which kinds of microtubule dynamic perturbations are capable of rescuing spindle bipolarity in Eg5-inhibited cells and, importantly, if rescues happen through a direct readjustment of the force equilibrium or if a different bipolarization pathway is activated. In this study, we aimed to address

Correspondence to: Stefan Florian and Thomas U. Mayer; Email: stefan.florian@uni-konstanz.de and Thomas.U.Mayer@uni-konstanz.de

these questions to understand how the two pathways, motor-derived forces and regulated microtubule dynamics, contribute to spindle bipolarization.

Results

TOGp depletion enables spindle bipolarization in Eg5-inhibited cells. To reinvestigate the functional interdependence between microtubule dynamics and spindle bipolarity, we first analyzed if RNA-interference (RNAi)-mediated depletion of TOGp rescues Eg5 inhibition. TOGp is a member of the XMAP215 family of microtubule-binding proteins, and its depletion causes reduced microtubule growth rates accompanied by defects in centrosome maturation and chromosome alignment.[7,37-40] To ensure accurate quantification of bipolar spindle formation efficiency, we used live-cell imaging throughout this study, except for structural spindle studies, which required immunofluorescence analyses. For our initial analyses, we used HeLa cells stably expressing green fluorescent protein (GFP)-tagged histone 2B (H2B-GFP) and followed chromosomal morphology and arrangement through mitosis. Cells were defined as containing a bipolar spindle once chromosomes were arranged at the metaphase-plate, which was readily distinguishable from the ring-like arrangement of chromosomes around monopolar spindles. Depletion of TOGp followed by incubation with VS83, a more potent derivate of the Eg5 inhibitor monastrol,[41] significantly restored spindle bipolarity, as indicated by an increase in the percentage of mitotic cells forming bipolar spindles from 17% (GL2-RNAi control) to 44% (**Fig. 1A**). To directly follow spindle formation under these conditions, we used a HeLa cell clone stably expressing α-tubulin-GFP and CENP-A-GFP as spindle morphology and kinetochore markers, respectively (TC21),[42] (**Fig. 1B and Movies S1–S3**). In unperturbed cells (DMSO-treated), spindle formation followed the expected sequence of events: centrosome separation started in prophase or prometaphase and occurred through a smooth continuous movement. Increased centrosomal microtubule nucleation started briefly before nuclear envelope breakdown and the two centrosomes constituted the only visible source of microtubule nucleation (**Fig. 1B and Movie S1**). As expected, when Eg5 was inhibited, microtubule nucleation at centrosomes was not affected, but centrosomes did not separate and formed a monopolar spindle (**Fig. 1B and Movie S2**), inducing mitotic arrest. Intriguingly, in cells depleted of TOGp and treated with VS83, we observed the formation of supernumerary nucleation centers scattered in the vicinity of chromosomes immediately after nuclear envelope breakdown (**Fig. 1B and Movie S3**). Notably, these supernumerary nucleation centers were clearly distinguishable from centrosomes, which were visible as sources of nucleation before nuclear envelope breakdown. Interestingly, we observed that the two centrosomes did not separate initially while the supernumerary nucleation centers formed a second or third pole resulting in bipolar-like or multipolar spindles. To ensure that the accessory poles formed after nuclear envelope breakdown are, indeed, of acentrosomal nature rather than centrosomal fragments or supernumerary centrosomes, we stained for centrosome-specific markers in prophase cells immediately after nuclear envelope breakdown (as assessed by DNA morphology). In prophase cells depleted of TOGp and treated with VS83, we observed two nucleation centers that were positive for both centrin and pericentrin and, importantly, additional distant nucleation centers that were negative for both markers, confirming the acentrosomal nature of the supernumerary poles (**Fig. 1C**). In summary, these data suggest that spindle assembly in cells depleted of TOGp and treated with VS83 involves an intermediary phase characterized by a mix of centrosomal and acentrosomal poles. After centrosomal and acentrosomal nucleation centers coalesced to form an intermediate multipolar structure, it was difficult to follow the fate of centrosomes in real-time in TC21 cells. Therefore, we determined by immunofluorescence analyses the final position of centrosomes at the end of the bipolarization process. In over 70% of bipolar spindles that formed in VS83-treated TOGp-RNAi cells, both poles stained positively for the centrosomal markers centrin and pericentrin (**Fig. 1D**). Protein gel blotting confirmed that siRNA transfection resulted in efficient depletion of TOGp from HeLa cells (**Fig. 1E**). This observation together with our live analyses suggest that TOGp-depletion restores spindle bipolarity by a mechanism where, initially, intermediate structures composed of centrosomal and acentrosomal poles form which then reorganize into bipolar spindles with centrosomes at each of the two spindle poles.

Low-dose nocodazole rescues Eg5 inhibition. Several roles in organizing spindle shape and function have been reported for TOGp.[7,38,43-45] To test if spindle rescue by TOGp depletion is, indeed, caused by altered microtubule dynamics rather than by perturbation of other processes, we tried to replicate the effect using the microtubule poison nocodazole. For these experiments, we used 50 nM nocodazole, a dose known to suppress microtubule dynamics[46] and to induce chromosome alignment defects similar to the ones observed in TOGp-RNAi cells.[47] Indeed, live-analyses revealed that the presence of 50 nM nocodazole

Figure 1 (See opposite page). TOGp depletion enables bipolar spindle formation in Eg5-inhibited cells. (A) HeLa H2B-GFP cells were transfected with luciferase (GL2, control) or TOGp siRNA duplexes for 30 h and then treated with the Eg5 inhibitor VS83. Cells were imaged for the subsequent 18 h and the fraction of mitotic cells that reached metaphase was quantified by live-cell microscopy. The bar plot represents the mean ± 1 standard error of the mean of three experiments. (B) Representative time lapse images of HeLa cells expressing α-tubulin-GFP and CENP-A-GFP that were treated as indicated following the same protocol as in (A). Time of nuclear envelope breakdown (NEB) was set to zero minutes. Note the non-centrosomal microtubule nucleation center that appears immediately after NEB in the TOGp-depleted cell only. Cartoons are provided to illustrate the spindle formation process. Nucleation centers and polar structures are color-coded as indicated. **Movies S1–S3** display the full sequences. (C) Immunofluorescence images of a VS83-treated HeLa cell inducibly expressing centrin GFP and depleted of TOGp, demonstrating that supernumerary nucleation centers are negative for the centrosomal proteins centrin and pericentrin. Cells were stained for the indicated antigens. (D) Representative immunofluorescence images of bipolar spindles formed under the indicated conditions using the same cell line and protocol as in (C). Scale bars represent 15 μm. (E) HeLa cells were transfected for 40 h with 25 nM TOGp siRNA or control siRNA, and the amount of TOGp and Eg5 protein in whole-cell lysate was assessed by protein gel blot.

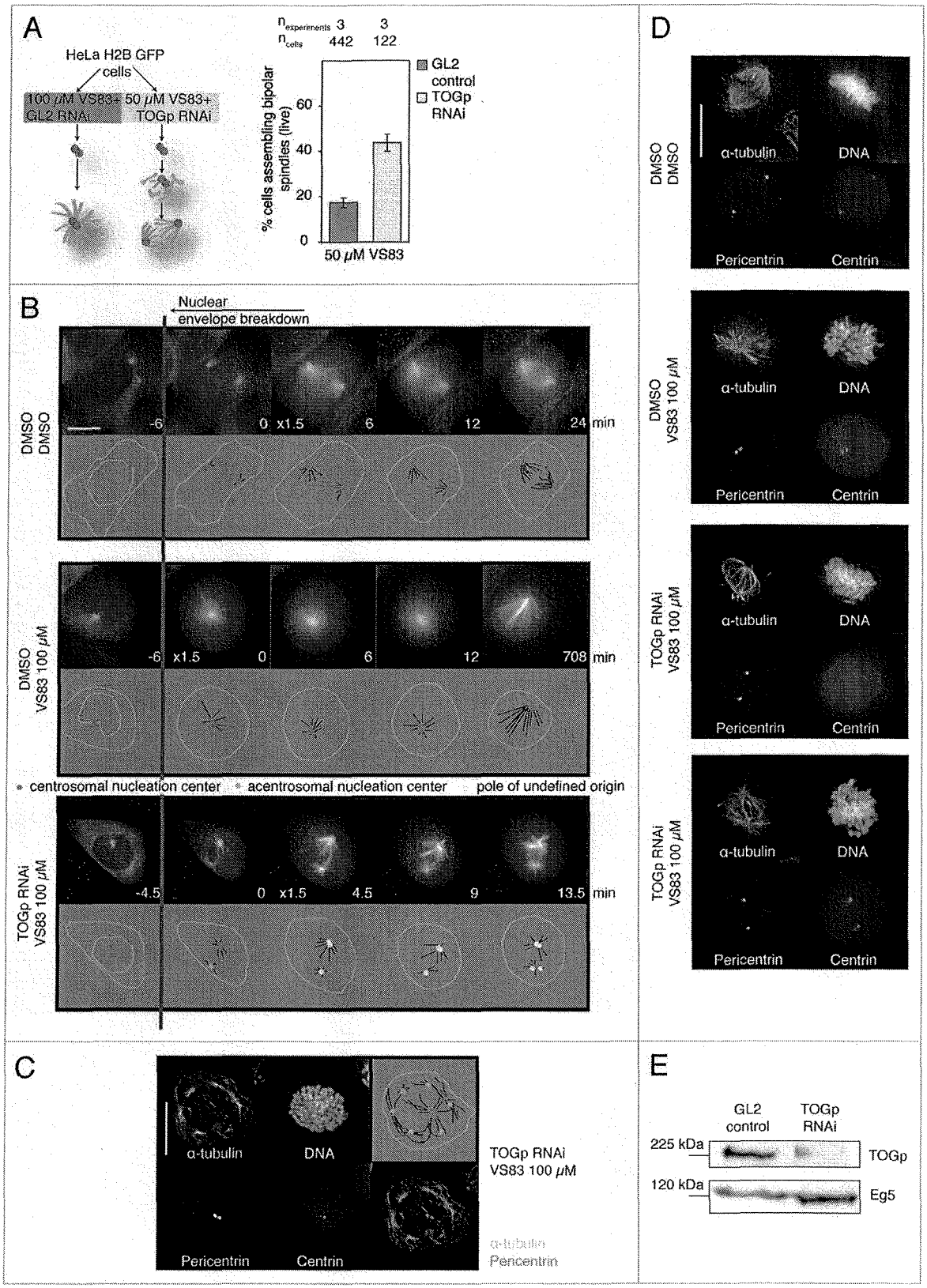

Figure 1. For figure legend, see page 3534.

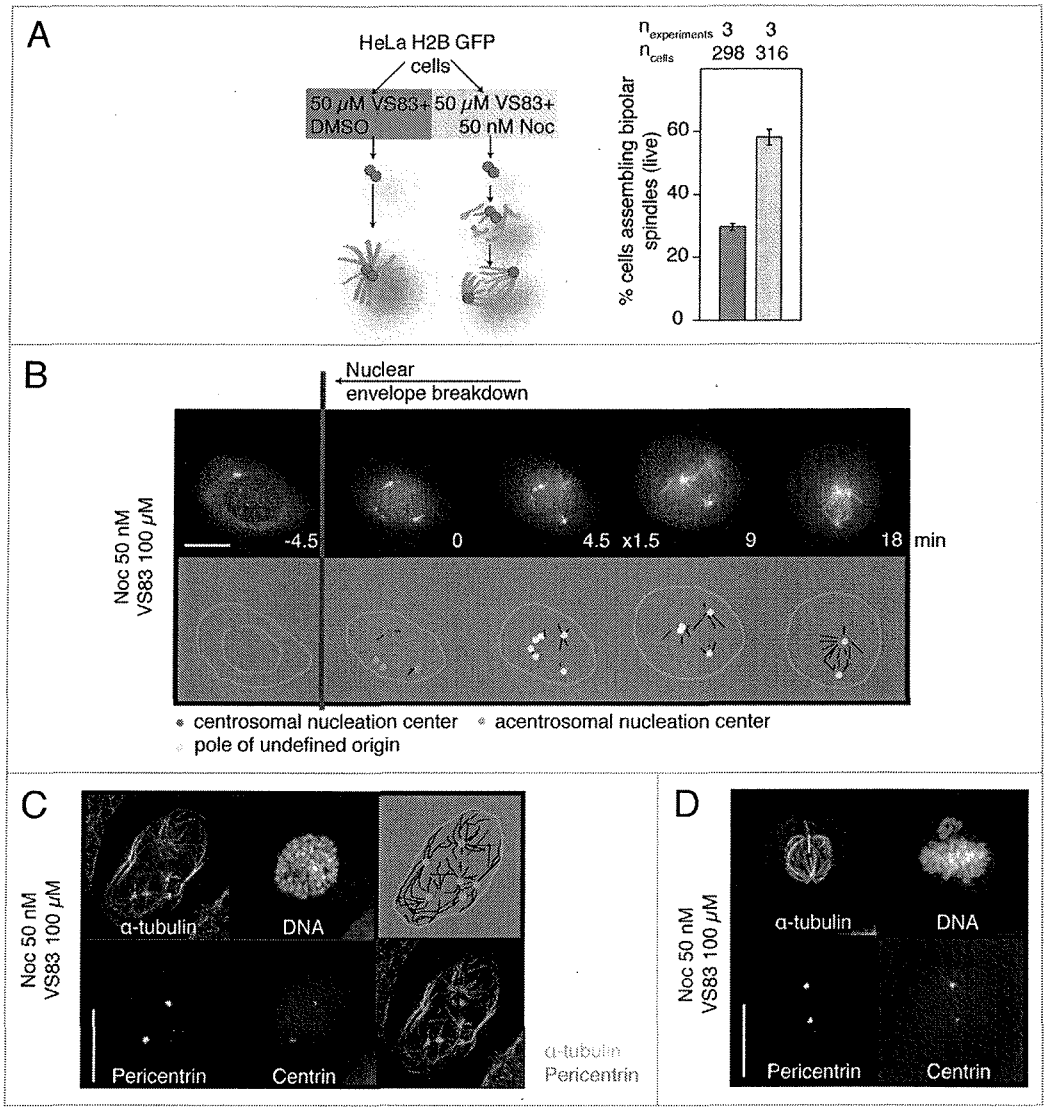

Figure 2. Low-dose nocodazole treatment enables bipolar spindle formation in Eg5-inhibited cells. (A) HeLa H2B-GFP-cells were simultaneously treated with the Eg5 inhibitor VS83 and nocodazole and imaged for the subsequent 18 h. The fraction of mitotic cells that reached metaphase was quantified by live-cell microscopy. The bar plot represents the mean ± 1 standard error of the mean of three experiments. (B) Representative time lapse images of HeLa-cells expressing α-tubulin-GFP and CENP-A-GFP that were treated as indicated following the same protocol as in (A). Time of nuclear envelope breakdown (NEB) was set to zero minutes. Note the non-centrosomal microtubule nucleation centers that appear immediately after NEB. Cartoons are provided to illustrate the spindle formation process. Nucleation centers and polar structures are color-coded as indicated. **Movie S4** contains the full movie sequence. (C) Immunofluorescence images of a representative VS83 and nocodazole treated HeLa-cell inducibly expressing centrin GFP and demonstrating that supernumerary nucleation centers are negative for the centrosomal proteins centrin and pericentrin. Cells were stained for the indicated antigens. (D) Representative immunofluorescence image of a bipolar spindle formed under the indicated conditions using the same cell line and protocol as in (C). Scale bars represent 15 μm.

improved bipolar spindle formation in VS83-treated cells from 30% in the DMSO/VS83-control to 58% (**Fig. 2A**). Thus, nocodazole mimics the effect of TOGp depletion, indicating that, under both conditions, altered microtubule dynamics account for restoration of spindle bipolarity in VS83-treated cells. Notably, an optimal effect was only observable in a narrow window of nocodazole concentrations ranging from 40 nM to 60 nM, and no effect was observed above 75 nM, providing an explanation as to why a previous study using 100 nM nocodazole did not observe spindle rescue in Eg5-inhibited cells.[21] Imaging spindle formation in TC21 cells treated with VS83 and nocodazole revealed patterns of events highly reminiscent to TOGp-depleted cells: nuclear envelope breakdown was accompanied by the appearance of acentrosomal nucleation centers, which first converged into a multipolar structure that was then was reshaped into a bipolar spindle (**Fig. 2B and Movie S4**). Immunofluorescence analysis of

early mitotic cells confirmed that supernumerary nucleation centers were of acentrosomal nature (**Fig. 2C**). Notably, immunofluorescence characterization of spindles formed in Eg5-inhibited and nocodazole-treated cells revealed that in over 90% of bipolar spindles, both poles contain centrosomes (**Fig. 2D**). In summary, these experiments suggest that both nocodazole addition and TOGp depletion rescue spindle bipolarity through a common mechanism that relies on modulated microtubule dynamics.

Perturbed microtubule dynamics are required during initial stages of bipolarization. Next, we addressed the functionality of spindles assembled under rescue conditions. For these experiments, we used nocodazole, because its fast and reversible mode of action allowed flexible and complex experimental setups. First, we investigated if nocodazole-induced spindles are functional. Analyses of cells co-treated with 100 μM VS83 and 50 nM nocodazole by time-lapse microscopy revealed that 88% of the spindles performed anaphase. However, compared with control cells (DMSO/DMSO control), these spindles required much longer both to align chromosomes at the spindle equator and to enter anaphase: 137 min and 16 min from nuclear envelope breakdown to metaphase plate formation for VS83/nocodazole and DMSO/DMSO-control, respectively; 219 min and 25 min from metaphase to anaphase onset, respectively (**Fig. 3A**). In addition to the delay in chromosome alignment, we also observed frequent lagging chromosomes in nocodazole-treated spindles which entered anaphase. Thus, under rescue conditions, spindles are able to accomplish the primary task of chromosome segregation, albeit less efficiently than wild-type spindles.

Notably, we observed that vinblastine, a microtubule drug widely used as a chemotherapeutic agent,[47,48] can also rescue bipolar spindle formation (**Fig. 3B**). Similar to nocodazole-induced rescue, analyses of HeLa cells stably co-expressing mEGFP-tagged α-tubulin and mCherry-H2B[49] revealed an optimal rescue within a tight dose range of 0.9 to 1.5 nM vinblastine which was associated with the formation of acentrosomal spindle poles. Rescue efficiency was even higher than with nocodazole, resulting in 70% of Eg5-inhibited mitotic cells forming a bipolar spindle in the presence of 1.3 nM vinblastine compared with only 16% in DMSO treated control cells.

Next, we wanted to gain insights into the mechanism underlying nocodazole-induced spindle rescue. In unperturbed mammalian cells, Eg5 is essential only during the early steps of centrosome separation and inhibition of Eg5 in a cell with preformed bipolar spindles normally does not lead to spindle collapse.[23,28,32,33] Thus, Eg5 is essential for the establishment but not maintenance of spindle bipolarity. We designed a series of experiments to see if the same conditions apply to perturbed microtubule dynamics in Eg5-inhibited cells. First, we induced monopolar spindles in TC21 cells by VS83-treatment and then followed the structure of these spindles after the addition of 50 nM nocodazole or DMSO (control) by time-lapse microscopy. Notably, compared with the DMSO-control, addition of nocodazole did not increase the percentage of monopolar spindles that reorganized into bipolar structures (**Fig. 3C** and left part). Thus, in contrast to reactivation of Eg5, perturbation of microtubule dynamics after a monopolar spindle has formed is not able to convert it into a bipolar spindle, suggesting that the presence of nocodazole might be essential during the initial phase of spindle assembly to rescue spindle bipolarity. To corroborate this hypothesis, we induced the disassembly of preformed monopolar spindles by transferring Eg5-inhibited TC21 cells for one hour to 4°C and then, after the addition of nocodazole or DMSO to the VS83-containing media, we initiated spindle reformation by shifting the cells back to 37°C. Due to the high precision of the microscope stage, we were able to relocate individual cells after the cold-induced disassembly of monopolar spindles. Interestingly, while in the DMSO control, nearly all (except for 1%) of the monopolar spindles remained monopolar, in the presence of 50 nM nocodazole, 28% of the initially monopolar spindles converted to the bipolar state (**Fig. 3C**, right part). Thus, while cold-treatment made it more difficult for Eg5-inhibited cells to assemble bipolar spindles (20% at constant 37°C compared with 1% after cold treatment), the net improvement in bipolar spindle formation caused by nocodazole treatment remained approximately constant (compare with **Figs. 2A and 4**). Consistent with our previous observations, cells recovering from cold-induced microtubule depolymerization in the presence of nocodazole formed supernumerary nucleation centers in the vicinity of chromosomes that subsequently coalesced into bipolar structures. As expected, these centers were not detectable in the DMSO control. From these observations, we conclude that perturbed microtubule dynamics are required during the initial assembly phase of spindles to compensate for Eg5 inhibition.

Nocodazole is not required to maintain bipolarity in Eg5-inhibited cells. Next, we investigated if the presence of nocodazole during the initial phase of spindle assembly is not only required, but actually sufficient, to restore bipolarity in Eg5-inhibited cells. To test this, we co-treated HeLa H2B-GFP cells with 100 μM VS83 and 50 nM nocodazole to allow bipolar spindle formation and then monitored cells with bipolar spindles after washout of nocodazole or both nocodazole and VS83 by time-lapse microscopy (**Fig. 3D**). Upon washout of nocodazole and VS83, none of the initially bipolar spindles collapsed, and 97% entered anaphase. Importantly, even after washout of only nocodazole (thus keeping Eg5 inhibited), we did not detect a single bipolar spindle collapsing and, furthermore, 91% of these cells entered anaphase within 77 min on average, which is about two thirds faster than the 217 min rescued spindles require to enter anaphase in the continuous presence of nocodazole (**Fig. 3A**). Thus, these data suggest that nocodazole is not only dispensable for bipolarity once bipolar spindles have formed in Eg5-inhibited cells, but negatively affects the functionality of these spindles. This implies that bipolar spindles that form under rescue conditions in Eg5-inhibited cells do not require altered microtubule dynamics to maintain their bipolar structure and functionality. This observation cannot be explained by models which suggest that rescue is mediated through the modulation of the microtubule overlap zone, because such models predict the collapse of bipolar spindles once the microtubule-perturbing factor has been removed.[23] Thus, nocodazole might rescue bipolar spindle formation through a distinct mechanism.

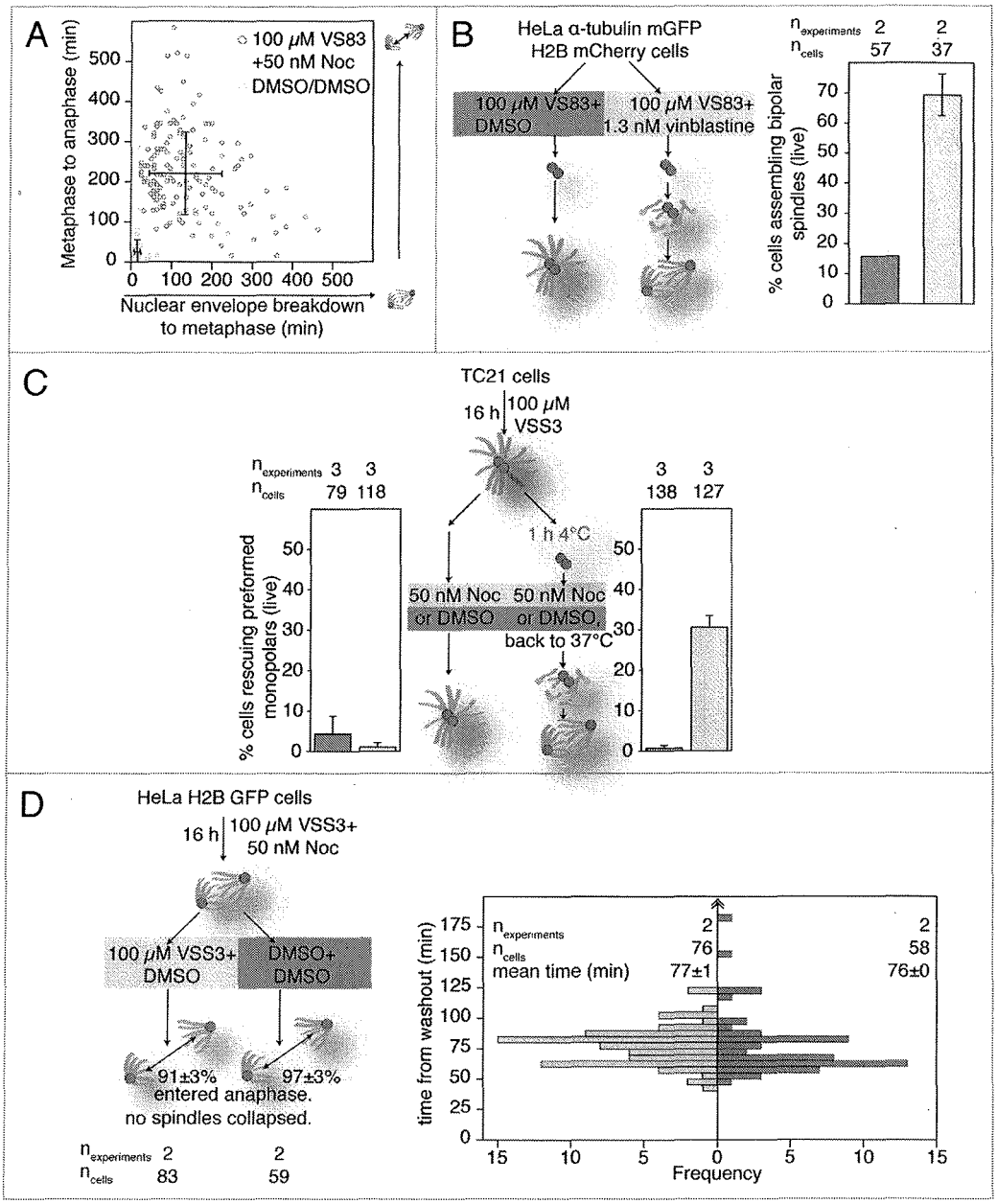

Figure 3. Functional characterization of rescued bipolar spindles. (A) HeLa H2B-GFP cells were simultaneously treated with the Eg5 inhibitor VS83 and nocodazole (brown circles) or solvent control (DMSO/DMSO, yellow circles) and imaged for the subsequent 18 h. The times from NEB to metaphase plate formation (x-axis) and from metaphase plate formation to anaphase entry (y-axis) were measured. Error bars represent ± 1 standard deviation and intersect each other at the population mean. The plot shows the pooled individual cells from three experiments. (B) HeLa cells stably expressing mEGFP tagged α-tubulin and mCherry-tagged Histone 2B were simultaneously treated with the Eg5 inhibitor VS83 and vinblastine and imaged for the subsequent 18 h. The fraction of mitotic cells that reached metaphase was quantified by live-cell microscopy. The bar plot represents the mean ± 1 standard error of the mean of two experiments. (C) Left plot: HeLa cells expressing α-tubulin-GFP and CENP-A-GFP treated with 100 μM VS83 and then 50 nM nocodazole or DMSO according to the scheme. In three experiments, the fraction of preformed monopolar spindles that became bipolar upon addition of nocodazole or DMSO was quantified. Right plot: The same experiment was repeated and quantified in the same way as on the left, but an 1-h microtubule depolymerization step at 4°C was introduced before nododazole addition to induce de novo spindle formation in mitotic cells that previously contained spindles arrested in the monopolar state. In both plots, only the fate of initially monopolar spindles was followed. (D) HeLa H2B-GFP cells were simultaneously treated with nocodazole and the Eg5 inhibitor VS83 and rescued bipolar spindles allowed to accumulate for 16 h. Then, either nocodazole or both compounds were washed out and replaced with solvent control (DMSO), and initially bipolar spindles were followed for 13 h. The right plot shows histograms and descriptive statistics of the time the spindles required to enter anaphase after compound washout. Descriptive statistics represent the means ± 1 standard error of the mean from two experiments.

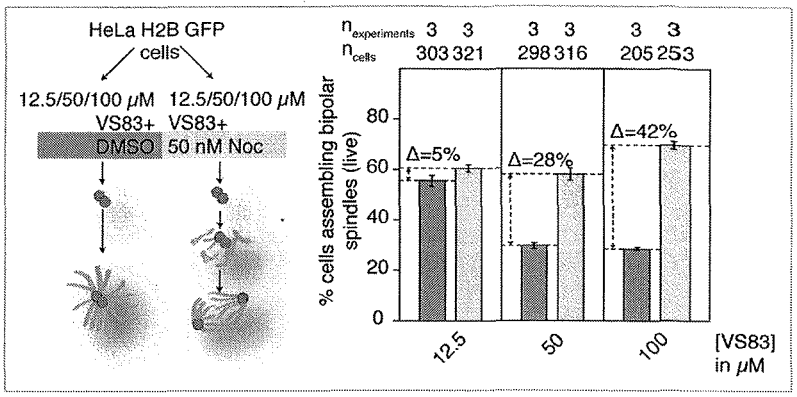

Figure 4. Low-dose nocodazole and Eg5 activity enable bipolar spindle formation through mutually exclusive pathways. HeLa H2B-GFP cells were simultaneously treated with the indicated doses of the Eg5 inhibitor VS83 and nocodazole and imaged for the subsequent 18 h. The fraction of mitotic cells that reached metaphase was quantified by live-cell microscopy. The bar plot represents the mean ± 1 standard error of the mean of three experiments. Note that lower concentrations of Eg5 inhibitor have a negative effect on the net improvement in bipolar spindle formation induced by nocodazole treatment.

Nocodazole-induced rescue mechanism is more efficient with lower Eg5 activity. Existing models treat pole separation as the consequence of multiple individual forces pushing or pulling poles along the spindle axis, which finally results in the formation of bipolar spindles whose constant length and shape reflect the balance of all forces acting on the spindle.[50,51] Eg5, for example, pushes antiparallel microtubules outward, and this explains why its inhibition prevents pole separation.[26,52] In line with this model, it has been reported that reducing inward forces by co-depletion of the Eg5 antagonist dynein restores spindle bipolarity by a process that seems to rely on residual Eg5 activity.[53] These observations prompted us to analyze if nocodazole rescues spindle bipolarity through a similar mechanism, i.e., by strengthening outward forces or reducing inbound forces. If this applies, raising the dose of Eg5 inhibitor should decrease the efficacy of nocodazole to restore spindle bipolarity. As expected, time-lapse analyses of DMSO-control cells revealed that increasing VS83 concentrations resulted in decreasing numbers of mitotic cells that assembled bipolar spindles (Fig. 4). Surprisingly and in contrast, in the presence of nocodazole an 8-fold increase in VS83 concentration had only a small effect on the absolute percentage of mitotic cells assembling bipolar spindles, 61%, 58% and 70% at 12.5 μM, 50 μM and 100 μM, respectively, but significantly improved the net efficacy of nocodazole to rescue spindle bipolarity when compared with DMSO/VS83-treated cells to Δ5%, Δ28% and Δ43%, respectively (Fig. 4). Thus, these data suggest that nocodazole does not intervene with the balance of forces between Eg5 and its antagonists and rescues spindle bipolarity through a mechanism clearly distinct from the one of dynein depletion.

Nocodazole enables Hklp2/Kif15 to assemble bipolar spindles. The plus end-directed kinesin Hklp2/Kif15 is required to maintain, but is not able to establish, spindle bipolarity when Eg5 is inhibited.[32,33] Thus, Hklp2/Kif15 cannot complement the function of Eg5 in centrosome separation during spindle assembly, but shares redundant functions with Eg5 once bipolarity is established. Having observed that the efficacy of nocodazole in spindle rescue is not affected by increased Eg5 inhibition we speculated that low doses of nocodazole might create conditions that enable Hklp2/Kif15 to replace Eg5 in pole separation. To test this hypothesis, we repeated the nocodazole rescue experiments in VS83-treated cells depleted of Hklp2/Kif15 or control RNAi-cells (GL2-RNAi) and followed spindle assembly by live microscopy. Compared with GL2-RNAi cells, depletion of Hklp2/Kif15 dramatically reduced the percentage of mitotic cells that formed bipolar spindles from 51% to 4% (Fig. 5A). This effect was reproducible with four different short interfering RNA duplexes targeting Hklp2/Kif15 mRNA. Importantly, we observed that the depletion of Hklp2/Kif15 did not prevent the formation of nocodazole-induced acentrosomal nucleation centers, which were clearly visible upon nuclear envelope breakdown (Fig. 5B). Protein gel blotting confirmed that siRNA transfection resulted in a considerable reduction of Hklp2/Kif15 levels in HeLa cells (Fig. 5C). Thus, nocodazole-induced spindle rescue relies on Hklp2/Kif15 activity, suggesting that altered microtubule dynamics during spindle assembly enables Hklp2/Kif15 to compensate for Eg5 inhibition.

Discussion

In the last decade, a number of studies were performed to identify molecular perturbations that enable bipolar spindle formation when Eg5 is inhibited. These studies were motivated by the aim to (1) understand how Eg5 contributes to bipolarization and (2) identify backup mechanisms cells can resort to if physiological spindle formation fails. Previous studies have focused on two main groups of perturbations that counteract Eg5 inhibition: inhibition of molecular motors and perturbation of microtubule dynamics. The results are, in all but one case,[33] interpreted in the context of the push-pull model of spindle formation inspired from muscle sarcomers.[26] This is a very elegant and intuitive model, and it was developed based on insights from in vitro observations that some molecular motors can cross-link and move microtubules. It interprets bipolarization as the result of pushing and pulling forces exerted by motors that cross-link antiparallel microtubules at the spindle equator. If Eg5 is inhibited, minus end-directed antagonistic motors become dominant and prevent pole separation. Accordingly, attenuating antagonistic motors like HSET or dynein[53-55] or strengthening synergistic motors like Hklp2/Kif15[32,33] can compensate for reduced Eg5 activity and restore the equilibrium of forces. Reportedly, microtubule dynamics can indirectly influence this equilibrium through modulation of microtubule length and, thus, by varying the zone where cross-linking motors can act.[23]

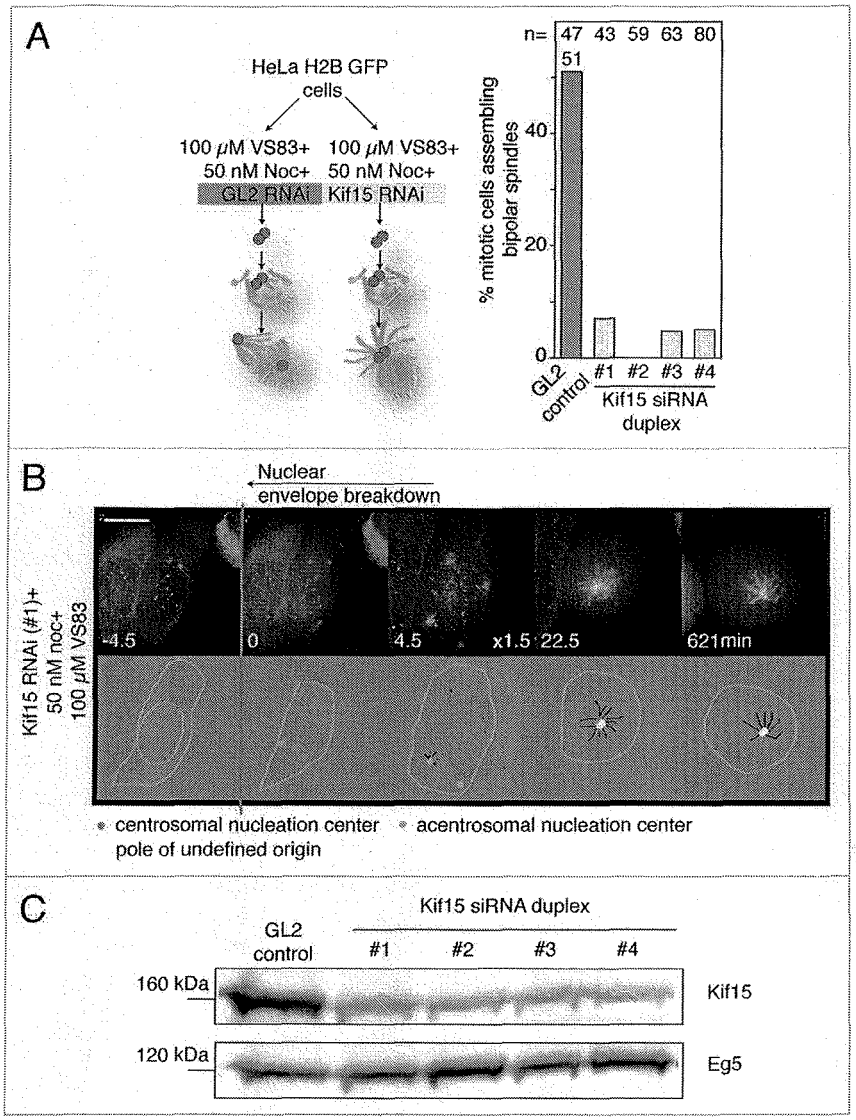

Figure 5. Rescued spindle formation depends on Hklp2/Kif15. (A) HeLa cells stably expressing α-tubulin-GFP and CENP-A-GFP were transfected with 1 out of 4 different RNAi oligonucleotides against Hklp2/Kif15 or control (GL2) RNAi and incubated for 30 h. Then, cells were simultaneously treated with the Eg5 inhibitor VS83 and nocodazole and imaged for the subsequent 18 h. The fraction of mitotic cells that reached metaphase was quantified by live-cell microscopy. The bar plot represents the results from one experiment. (B) Representative time lapse images of HeLa cells expressing α-tubulin-GFP and CENP-A-GFP that were treated as indicated following the same protocol as in (A). Time of nuclear envelope breakdown (NEB) was set to zero minutes. Note the non-centrosomal microtubule nucleation centers that appear immediately after NEB. Cartoons are provided to illustrate the spindle formation process. Nucleation centers and polar structures are color-coded as indicated. **Movie S5** shows the full sequence. (C) HeLa cells were transfected for 40 h with 25 nM Kif15 siRNA (four different oligonucleaotides) or control siRNA, and the amount of Kif15 and Eg5 protein in whole-cell lysate was assessed by protein gel blot.

In this study, we established that nocodazole (in lower doses than used by Ganem et al.) enables spindle formation in Eg5-inhibited cells. A second treatment, TOGp depletion, gave similar results. In contrast to previous work, we looked at spindle bipolarity not only as a morphological property, but we also analyzed the functional properties of resulting spindles and the sequence of events leading to bipolar spindle formation. Live analysis of spindle formation revealed that, unexpectedly, the process of spindle formation under rescue conditions seems to differ conceptually from normal spindle formation. It starts with unseparated centrosomes, followed by the formation of multiple acentrosomal nucleation centers upon nuclear envelope breakdown. Both centrosomal and acentrosomal nucleation centers form an intermediate structure that is restructured into a bipolar spindle via a mechanism involving pole focusing. Interestingly, during this restructuring process, centrosomes are correctly distributed so that the final spindle contains two centrosomal poles and, upon washout of nocodazole, quickly enters anaphase. This sequence of events is reminiscent of spindle formation in meiotic systems. Mouse oocytes lack centrosomes and thus rely on acentrosomal microtubule organizing centers, which converge to form a bipolar spindle after passing through a multipolar step in a manner reminiscent of the one observed here upon depletion of TOGp or nocodazole treatment.[56,57] Notably, during development of mouse embryos, the mechanism of spindle assembly changes profoundly from an acentrosomal to a centrosomal process, and the maintenance of spindle bipolarity becomes independent of Eg5 activity,[36] indicating that somatic cells can integrate different routes of spindle assembly. The potential to switch the mechanism of spindle assembly has also been observed in mammalian and Drosophila tissue culture cells, which form acentrosomal spindles if centrosomes have been experimentally inactivated.[58-60]

While it would be possible to extend existing models, e.g., stating that microtubule dynamics affect the overlap zone and, thus, the strength of Eg5-derived forces,[23] to explain some of our observations, the following line of evidence suggests that an acentrosomal spindle formation pattern is essential for bipolarization under rescue conditions (a suggested model is outlined in **Fig. 6**): first, the appearance of acentrosomal poles strongly correlates with spindle rescue; i.e., in over 90% of the cells that assembled bipolar spindles in the presence of 50 nM nocodazole and 100 μM VS83 we clearly observed supernumerary nucleation centers in the vicinity

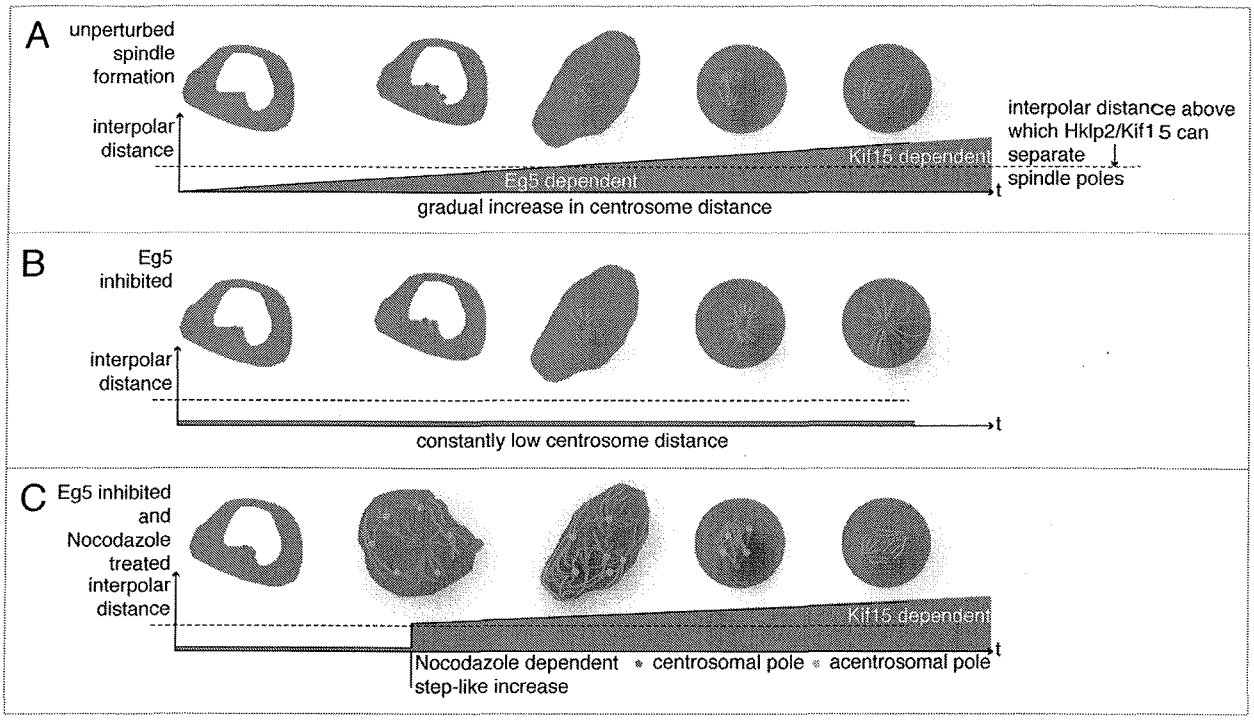

Figure 6. A model for Kif15-dependent rescued spindle formation. (A) Unperturbed spindle formation relies on Eg5 for initial centrosome separation which, once a certain threshold interpolar distance is reached, allows Hklp2/Kif15 to fully separate spindle poles. (B) If Eg5 is inhibited, initial centrosome separation is not possible. Therefore the threshold interpolar distance is not reached, thus preventing Hklp2/Kif15 from contributing to pole separation. (C) Perturbation of microtubule dynamics through TOGp depletion or low-dose microtubule drugs like vinblastine and nocodazole induce the formation of accessory acentrosomal poles at NEB, thus creating an intermediate multipolar structure with an average interpolar distance above the threshold. This, along with modulated dynamic properties of microtubules, allows Hklp2/Kif15 to reshape this structure into a bipolar spindle.

of chromosomes upon nuclear envelope breakdown. As shown by our immunofluorescence analyses and supported by previous reports in references 7 and 61, these nucleation centers lack centrosomal components and, therefore, are acentrosomal. Second, while not being able to rescue preformed monopolar spindles, the presence of nocodazole during spindle assembly is sufficient to restore bipolarity in Eg5-inhibited cells (**Fig. 3C**). If constant perturbation of microtubule dynamics was required to maintain the push-pull equilibrium on antiparallel microtubules,[23] one would predict that nocodazole has to be present even after bipolarity has been established. As shown in **Figure 3D**, in Eg5-inhibited cells, spindles not only retained their bipolar shape upon nocodazole washout, but segregated chromosomes with improved kinetics compared with rescued spindles in the continuous presence of nocodazole, demonstrating that nocodazole is dispensable once bipolarity is established. Third, nocodazole treatment enables Hklp2/Kif15 to mediate spindle pole separation (**Fig. 5**). In references 32 and 33, it was shown that physiological levels of Hklp2/Kif15 can only contribute to spindle assembly once spindle poles have reached a minimum distance from each other. Since acentrosomal centers already emerge scattered around chromosomes (**Figs. 1BC, 2BC and 5B**), it is tempting to speculate that the initial Eg5-dependent process is bypassed under rescue conditions and Hklp2/Kif15 takes it from there to fully assemble bipolar spindles. In line with this postulated order of events, we observed that Hklp2/Kif15 depletion did not interfere with the formation of nocodazole-induced acentrosomal nucleation centers (**Fig. 5B**) but with the transition of the initial structures into bipolar spindles. Fourth, nocodazole-induced rescue is more effective with increasing Eg5 inhibition (**Fig. 4**). If nocodazole treatment would re-equilibrate the balance of forces, one would predict that increasing inhibition of Eg5 would result in a decrease in the percentage of mitotic cells that assemble bipolar spindles at a given nocodazole concentration. However, we observed that increasing VS83 concentrations had not only no significant effect on the absolute percentage of bipolar spindles forming at 50 nM nocodazole, but actually increased the net efficacy of nocodazole when compared with VS83/DMSO-control cells. Thus, our data suggest that spindle rescue by nocodazole occurs via a process that is mechanistically distinct from Eg5-mediated pole separation. A shift from an exclusively centrosome-driven mechanism toward an acentrosomal nucleation center-assisted spindle formation process upon nocodazole treatment or TOGp depletion would satisfactorily explain both the unique characteristics of spindle assembly we observed under rescue conditions and the detected differences from unperturbed spindle formation.

Our finding that modulated microtubule dynamics can replace Eg5 activity might also have important implications

for the design and evaluation of future cancer therapies. Eg5 inhibitors have been shown to kill tumor cells and inhibit tumor growth[62,63] and, consequently, are currently evaluated in clinical trials. In these studies, Eg5 inhibitors are frequently combined with microtubule drugs or administered to patients pre-treated with microtubule drugs.[64] Given that alterations in microtubule dynamics are a common mechanism responsible for the resistance of tumor cells to such drugs,[65-69] our insights suggest that cells resistant to microtubule drugs might also be insensitive to drug-induced inhibition of Eg5. Interestingly, we observed that vinblastine, a microtubule drug widely used in chemotherapy,[48] restores spindle bipolarity in Eg5-inhibited cells. However, this effect might be specific for the mode of action of the applied microtubule drug, since we did not observe spindle rescue in Eg5-inhibited cells by low doses of paclitaxel, another chemotherapeutic agent that binds to microtubules at a site distinct from that of vinblastine,[48,70] suggesting that a careful matching of microtubule drugs with Eg5 inhibitors might improve therapeutic efficacy. Alternatively, therapeutic regimens combining Eg5 inhibitors with S phase-specific or p53-targeting drugs[71,72] rather than microtubule drugs might improve their therapeutic efficacy.

Materials and Methods

RNAi experiments. RNAi transfections were performed at 25 nM final concentration using HiPerfect (Qiagen) following the manufacturer's protocol. In 96-well plates, the reverse transfection protocol was used. Briefly, cells were plated directly on premixed HiPerfect and RNAi oligonucleotide. For experiments performed on coverslips (larger scale transfections), cells were plated 24 h prior to transfection (traditional protocol). The following siRNA oligonucleotides were used:

Luciferase GL2 Duplex (D-001100-01-20), sense: 5'-CGU ACG CGG AAU ACU UCG AdT dT, antisense: 5'-UCG AAG UAU UCC GCG UAC GTd TdT (Dharmacon);

TOGp (SI00107961), target sequence: CAG CTT TAG TTT ACT AAA CTA (Qiagen);

Kif15 #1, sense: 5'-GCA UGU ACA GCU UCA AUU AUU, antisense: 5'-UAA UUG AAG CUG UAC AUG CUU (Dharmacon);

Kif15 #2, sense: 5'-CCG AGA GGA UCA AAU AAU AUU, antisense: 5'-UAU UAU UUG AUC CUC UCG GUU (Dharmacon);

Kif15 #3 (SI00125615), sense: r(GGA UUC CUA UGA CAA CUU A)dTdT antisense: r(UAA GUU GUC AUA GGA AUC C)dTdG (Qiagen);

Kif15 #4 (SI00125622), sense: r(GAC AGA GCU GAA UAA UUC A)dTdT antisense: r(UGA AUU AUU CAG CUC UGU C)dTdG (Qiagen).

DNA transfections (see section "cell lines") were performed with Fugene6 (Roche) according to the manufacturer's protocol.

Cell culture and cell lines. All cell lines were grown in Dulbecco's modified Eagle medium (Invitrogen, 61965-059) with 10% FCS (Invitrogen) at 37°C and 5% CO_2. For immunofluorescence experiments, we used HeLa cells (the same clone as in ref. 6) or a HeLa cell clone stably expressing GFP-tagged centrin in a tetracyclin-inducible manner. We derived this clone from HeLa cells using the FlpIn system from Invitrogen following the manufacturer's protocol. The pFRT/lacZeo vector was used to generate a stable, Zeocin-resistant, clone with only one FRT site. In a second step, we transfected this clone with pcDNA6/TR (for CMV promoter-driven expression of the Tet repressor) and isolated stable integrands with blasticidin and Zeocin. We then cloned the ORF of centrin 1 (NCBI acc. no. NM_004066) into a modified version of the pcDNA5/FRT vector with a C-terminal eGFP tag. This construct was cotransfected with pOG44 (for Flp recombinase expression) into the Tet-inducible FRT site containing HeLa clone. Positive clones were selected with Hygromycin B and analyzed for inducible expression of centrin 1-GFP by fluorescence microscopy. For all experiments, centrin-eGFP expression was induced with 16 ng/ml tetracyclin immediately after cells were seeded. For live cell imaging, we used either a HeLa clone stably expressing GFP-tagged histone H2B (as used in ref. 6), the TC21 HeLa clone coexpressing genomically integrated GFP-tagged α-tubulin and CENP-A,[42] kindly provided by Jan-Michael Peters, or a HeLa cell line stably expressing mEGFP-tagged α-tubulin and mCherry-tagged CENP-A kindly provided by Daniel Gerlich.[49]

Compounds. VS83[41] was synthesized by Vasiliki Sarli and was a kind gift of the lab of Athanassios Giannis. Nocodazole (M1404) and vinblastine (V1377) were purchased from Sigma.

Immunofluorescence staining and immunoblotting. Cells were fixed for 10 min in 4% formaldehyde, followed by a 10 min treatment with permeabilization buffer (200 mM PIPES at pH 6.8, 20 mM EGTA, 2 mM $MgCl_2$, 0.4% Triton X-100). Samples were washed twice with TBS + 0.1% Triton X-100 (TBST) and incubated for 1 h in TBST + 2% bovine-serum albumin (BSA). Antibodies were diluted in TBST + 2% BSA, and cells were incubated for 1 h, followed by two washing steps. Samples for high-resolution microscopy were mounted in 20 mM TRIS-HCl [pH 8.8], 0.5% phenylendiamine and 90% glycerol while fixed samples in 96-well plates were imaged in situ in TBST.

Immunoblots were performed using standard protocols as previously described in reference 6.

The following antibodies were used: mouse anti α-tubulin-FITC (clone DM1A, 1:500, F2168, Sigma), mouse anti α-tubulin (clone DM1A, 1:1,000, T6199, Sigma), rabbit anti pericentrin (1:1,000, ab4448, Abcam), Alexa Fluor 568 goat anti-mouse IgG (H + L) (1:1,000, A-11031, Invitrogen), Cy5-conjugated donkey anti-rabbit IgG (1:1,000, 711-175-152, Jackson Laboratories) and rabbit anti TOGp/chTOG (1:1,000, ab18320, Abcam). Rabbit antibodies were raised against bacterially expressed His-Eg5 (aa 1–369) and His-Hklp2/Kif15 (aa 371–643). Serum specificity was confirmed by RNAi experiments and immunoblotting (data not shown).

Microscopy. For low-resolution microscopy (all experiments quantified in this study) we used an ImageXpress Micro automated microscope (Molecular Devices) with heating option and a 5% CO_2 supply and 96-well plates with optical bottom (655090, Greiner). The objectives were a CFI Plan Fluor DLL 10x, N.A.: 0.3, W.D.: 16 mm or CFI Plan Fluor ELWD DM 20x C, N.A.: 0.45, W.D. 8.1-7.0 (Nikon). Cells were either imaged

live in RPMI media with 10% FCS at 37°C or fixed and stained with the respective antibodies before imaging. For quantification of movies in **Figures 1, 2 and 4**, only cells which entered mitosis at least 10 h before the end of the experiment were taken into account, to allow for enough time to accurately assess the fate of mitotic cells. This was necessary, because nocodazole-rescued cells require a long time to exit mitosis (max. 10 h). The experiment in **Figure 3C** was performed on a Zeiss Observer.Z1 inverted microscope with a heating chamber at 37°C in CO_2-independent medium (18045-054, Invitrogen) with 10% FCS on ibidi μ-Slides VI 0.4 (80606, ibidi) using a Plan-Apochromat 20x, N.A. 0.8, W.D. 0.55 (Zeiss). High-resolution images were acquired as z-stacks on a DeltaVision Core System using a Nikon PlanApo N 60x, N.A. 1.42, W.D. 0.15 oil objective for live cell imaging in CO_2 independent medium at 37°C or a UPlanSApo 100x, N.A. 1.4, W.D. 0.13 oil objective (both Olympus) for fixed samples. A CoolSnap HQ digital camera was used.

Software and image processing. High resolution images were acquired as z-stacks on a DeltaVision Core System and deconvolved using softWorx 4.0 software (Applied Precision). The additive-enhanced algorithm was used for deconvolution and iterated eight times (all other settings were default). Projections were generated using the "quick projection" function using the maximal intensity in the stack for each pixel. Images of fixed samples were exported as 16-bit grayscale tiff files for every channel, and the white point was readjusted using the Levels function in Adobe Photoshop CS3. After conversion to CMYK mode, the final images were converted to 8-bit and saved again as tiff files. The black and white points of projected frames of movies were adjusted, and they were exported as 8-bit jpeg image sequences with ImageJ v.1.44f.Data analysis and plotting were done in Aabel 3.0.4 (Gigawiz). Figures were assembled in Adobe Photoshop CS3 and Adobe Illustrator CS3 without any further adjustments to microscopy images.

Disclosure of Potential Conflicts of Interest

The authors declare that they have no conflict of interest.

Acknowledgments

We thank Olaf Stemmann for vectors and critical reading of the manuscript. We thank Lucia Sironi and the Mayer lab for fruitful discussions and critical reading of the manuscript. We are grateful to Jan-Michael Peters and Daniel Gerlich for providing cell lines and Vasiliki Sarli for VS83. We are also indebted to Anna Brendel for great technical support. This work was supported by a EU-Research Training Network Fellowship to S.F. (Understanding the Dynamic of Cell Division) and by the Deutsche Forschungsgemeinschaft (DFG).

Author Contributions

S.F. performed the experiments. S.F. and T.U.M. wrote the manuscript and designed the study.

References

1. Heald R, Walczak CE. Mitotic Spindle Assembly Mechanisms. The Kinetochore: From Molecular Discoveries to Cancer Therapy 2008; 231.
2. Walczak CE, Heald R. Mechanisms of mitotic spindle assembly and function. Int Rev Cytol 2008; 265:111-58; PMID:18275887; DOI:10.1016/S0074-7696(07)65003-7.
3. Mao Y, Varma D, Vallee R. Emerging functions of force-producing kinetochore motors. Cell Cycle 2010; 9:715-9; PMID:20160491; DOI:10.4161/cc.9.4.10763.
4. Jang CY, Fang G. The N-terminal domain of DDA3 regulates the spindle-association of the microtubule depolymerase Kif2a and controls the mitotic function of DDA3. Cell Cycle 2009; 8:3165-71; PMID:19738423; DOI:10.4161/cc.8.19.9724.
5. Manning AL, Bakhoum SF, Maffini S, Correia-Melo C, Maiato H, Compton DA. CLASP1, astrin and Kif2b form a molecular switch that regulates kinetochore-microtubule dynamics to promote mitotic progression and fidelity. EMBO J 2010; 29:3531-43; PMID:20852589; DOI:10.1038/emboj.2010.230.
6. Mayr MI, Hummer S, Bormann J, Gruner T, Adio S, Woehlke G, et al. The human kinesin Kif18A is a motile microtubule depolymerase essential for chromosome congression. Curr Biol 2007; 17:488-98; PMID:17346968; DOI:10.1016/j.cub.2007.02.036.
7. Barr AR, Gergely F. MCAK-independent functions of ch-Tog/XMAP215 in microtubule plus-end dynamics. Mol Cell Biol 2008; 28:7199-211; PMID:18809577; DOI:10.1128/MCB.01040-08.
8. Bheda A, Gullapalli A, Caplow M, Pagano JS, Shackelford J. Ubiquitin editing enzyme UCH L1 and microtubule dynamics: implication in mitosis. Cell Cycle 2010; 9:980-94; PMID:20160478; DOI:10.4161/cc.9.5.10934.
9. Wadsworth P, Khodjakov A. E pluribus unum: towards a universal mechanism for spindle assembly. Trends Cell Biol 2004; 14:413-9; PMID:15308207; DOI:10.1016/j.tcb.2004.07.004.
10. Rieder CL. Kinetochore fiber formation in animal somatic cells: dueling mechanisms come to a draw. Chromosoma 2005; 114:310-8; PMID:16270218; DOI:10.1007/s00412-005-0028-2.
11. Sawin KE, LeGuellec K, Philippe M, Mitchison TJ. Mitotic spindle organization by a plus-end-directed microtubule motor. Nature 1992; 359:540-3; PMID:1406972; DOI:10.1038/359540a0.
12. Kashina AS, Scholey JM, Leszyk JD, Saxton WM. An essential bipolar mitotic motor. Nature 1996; 384:225; PMID:8918872; DOI:10.1038/384225a0.
13. Kashina AS, Rogers GC, Scholey JM. The bimC family of kinesins: essential bipolar mitotic motors driving centrosome separation. Biochim Biophys Acta 1997; 1357:257-71; PMID:9268050; DOI:10.1016/S0167-4889(97)00037-2.
14. Mayer TU, Kapoor TM, Haggarty SJ, King RW, Schreiber SL, Mitchison TJ. Small molecule inhibitor of mitotic spindle bipolarity identified in a phenotype-based screen. Science 1999; 286:971-4; PMID:10542155; DOI:10.1126/science.286.5441.971.
15. Sharp DJ, Yu KR, Sisson JC, Sullivan W, Scholey JM. Antagonistic microtubule-sliding motors position mitotic centrosomes in Drosophila early embryos. Nat Cell Biol 1999; 1:51-4; PMID:10559864; DOI:10.1038/9025.
16. Kapoor TM, Mitchison TJ. Eg5 is static in bipolar spindles relative to tubulin: evidence for a static spindle matrix. J Cell Biol 2001; 154:1125-33; PMID:11564753; DOI:10.1083/jcb.200106011.
17. Kwok BH, Yang JG, Kapoor TM. The rate of bipolar spindle assembly depends on the microtubule-gliding velocity of the mitotic kinesin Eg5. Curr Biol 2004; 14:1783-8; PMID:15458652; DOI:10.1016/j.cub.2004.09.052.
18. Ferenz NP, Gable A, Wadsworth P. Mitotic functions of kinesin-5. Semin Cell Dev Biol 2010; 21:255-9; PMID:20109572; DOI:10.1016/j.semcdb.2010.01.019.
19. Holmfeldt P, Brattsand G, Gullberg M. Interphase and monoastral-mitotic phenotypes of overexpressed MAP4 are modulated by free tubulin concentrations. J Cell Sci 2003; 116:3701-11; PMID:12890753; DOI:10.1242/jcs.00685.
20. Maiato H, Fairley EA, Rieder CL, Swedlow JR, Sunkel CE, Earnshaw WC. Human CLASP1 is an outer kinetochore component that regulates spindle microtubule dynamics. Cell 2003; 113:891-904; PMID:12837247; DOI:10.1016/S0092-8674(03)00465-3.
21. Ganem NJ, Compton DA. The KinI kinesin Kif2a is required for bipolar spindle assembly through a functional relationship with MCAK. J Cell Biol 2004; 166:473-8; PMID:15302853; DOI:10.1083/jcb.200404012.
22. Laycock JE, Savoian MS, Glover DM. Antagonistic activities of Klp10A and Orbit regulate spindle length, bipolarity and function in vivo. J Cell Sci 2006; 119:2354-61; PMID:16723741; DOI:10.1242/jcs.02957.
23. Kollu S, Bakhoum SF, Compton DA. Interplay of microtubule dynamics and sliding during bipolar spindle formation in mammalian cells. Curr Biol 2009; 19:2108-13; PMID:19931454; DOI:10.1016/j.cub.2009.10.056.
24. Toso A, Winter JR, Garrod AJ, Amaro AC, Meraldi P, McAinsh AD. Kinetochore-generated pushing forces separate centrosomes during bipolar spindle assembly. J Cell Biol 2009; 184:365-72; PMID:19204145; DOI:10.1083/jcb.200809055.

25. Tillement V, Remy MH, Raynaud-Messina B, Mazzolini L, Haren L, Merdes A. Spindle assembly defects leading to the formation of a monopolar mitotic apparatus. Biol Cell 2009; 101:1-11; PMID:19055485; DOI:10.1042/BC20070162.
26. Kapitein LC, Peterman EJG, Kwok BH, Kim JH, Kapoor TM, Schmidt CF. The bipolar mitotic kinesin Eg5 moves on both microtubules that it crosslinks. Nature 2005; 435:114-8; PMID:15875026; DOI:10.1038/nature03503.
27. Tanenbaum ME, Medema RH. Mechanisms of centrosome separation and bipolar spindle assembly. Dev Cell 2010; 19:797-806; PMID:21145497; DOI:10.1016/j.devcel.2010.11.011.
28. Kapoor TM, Mayer TU, Coughlin ML, Mitchison TJ. Probing spindle assembly mechanisms with monastrol, a small molecule inhibitor of the mitotic kinesin, Eg5. J Cell Biol 2000; 150:975-88; PMID:10973989; DOI:10.1083/jcb.150.5.975.
29. Saunders WS, Hoyt MA. Kinesin-related proteins required for structural integrity of the mitotic spindle. Cell 1992; 70:451-8; PMID:1643659; DOI:10.1016/0092-8674(92)90169-D.
30. Blangy A, Lane HA, d'Herin P, Harper M, Kress M, Nigg EA. Phosphorylation by $p34^{cdc2}$ regulates spindle association of human Eg5, a kinesin-related motor essential for bipolar spindle formation in vivo. Cell 1995; 83:1159-69; PMID:8548803; DOI:10.1016/0092-8674(95)90142-6.
31. Roostalu J, Schiebel E, Khmelinskii A. Cell cycle control of spindle elongation. Cell Cycle 2010; 9:1084-90; PMID:20410686; DOI:10.4161/cc.9.6.11017.
32. Tanenbaum ME, Macurek L, Janssen A, Geers EF, Alvarez-Fernandez M, Medema RH. Kif15 cooperates with eg5 to promote bipolar spindle assembly. Curr Biol 2009; 19:1703-11; PMID:19818618; DOI:10.1016/j.cub.2009.08.027.
33. Vanneste D, Takagi M, Imamoto N, Vernos I. The role of Hklp2 in the stabilization and maintenance of spindle bipolarity. Curr Biol 2009; 19:1712-7; PMID:19818619; DOI:10.1016/j.cub.2009.09.019.
34. Miyamoto DT, Perlman ZE, Burbank KS, Groen AC, Mitchison TJ. The kinesin Eg5 drives poleward microtubule flux in *Xenopus laevis* egg extract spindles. J Cell Biol 2004; 167:813-8; PMID:15583027; DOI:10.1083/jcb.200407126.
35. Shirasu-Hiza M, Perlman ZE, Wittmann T, Karsenti E, Mitchison TJ. Eg5 causes elongation of meiotic spindles when flux-associated microtubule depolymerization is blocked. Curr Biol 2004; 14:1941-5; PMID:15530396; DOI:10.1016/j.cub.2004.10.029.
36. Fitzharris G. A shift from kinesin 5-dependent metaphase spindle function during preimplantation development in mouse. Development 2009; 136:2111-9; PMID:19465601; DOI:10.1242/dev.035089.
37. Charrasse S, Schroeder M, Gauthier-Rouviere C, Ango F, Cassimeris L, Gard DL, et al. The TOGp protein is a new human microtubule-associated protein homologous to the Xenopus XMAP215. J Cell Sci 1998; 111:1371-83; PMID:9570755.
38. Brouhard GJ, Stear JH, Noetzel TL, Al-Bassam J, Kinoshita K, Harrison SC, et al. XMAP215 is a processive microtubule polymerase. Cell 2008; 132:79-88; PMID:18191222; DOI:10.1016/j.cell.2007.11.043.
39. Cassimeris L, Becker B, Carney B. TOGp regulates microtubule assembly and density during mitosis and contributes to chromosome directional instability. Cell Motil Cytoskeleton 2009;
40. Slep KC. The role of TOG domains in microtubule plus end dynamics. Biochem Soc Trans 2009; 37:1002-6; PMID:19754440; DOI:10.1042/BST0371002.
41. Sarli V, Huemmer S, Sunder-Plassmann N, Mayer TU, Giannis A. Synthesis and biological evaluation of novel EG5 inhibitors. ChemBioChem 2005; 6:2005-13; PMID:16216042; DOI:10.1002/cbic.200500168.
42. Lénárt P, Petronczki M, Steegmaier M, Di Fiore B, Lipp JJ, Hoffmann M, et al. The small-molecule inhibitor BI 2536 reveals novel insights into mitotic roles of polo-like kinase 1. Curr Biol 2007; 17:304-15; PMID:17291761; DOI:10.1016/j.cub.2006.12.046.
43. Gergely F, Draviam VM, Raff JW. The ch-TOG/XMAP215 protein is essential for spindle pole organization in human somatic cells. Genes Dev 2003; 17:336-41; PMID:12569123; DOI:10.1101/gad.245603.
44. Cassimeris L, Morabito J. TOGp, the human homolog of XMAP215/Dis1, is required for centrosome integrity, spindle pole organization and bipolar spindle assembly. Mol Biol Cell 2004; 15:1580-90; PMID:14718566; DOI:10.1091/mbc.E03-07-0544.
45. Holmfeldt P, Stenmark S, Gullberg M. Differential functional interplay of TOGp/XMAP215 and the KinI kinesin MCAK during interphase and mitosis. EMBO J 2004; 23:627-37; PMID:14749730; DOI:10.1038/sj.emboj.7600076.
46. Vasquez RJ, Howell B, Yvon AM, Wadsworth P, Cassimeris L. Nanomolar concentrations of nocodazole alter microtubule dynamic instability in vivo and in vitro. Mol Biol Cell 1997; 8:973-85; PMID:9201709.
47. Jordan MA, Thrower D, Wilson L. Effects of vinblastine, podophyllotoxin and nocodazole on mitotic spindles. Implications for the role of microtubule dynamics in mitosis. J Cell Sci 1992; 102:401-16; PMID:1506423.
48. Jordan MA, Wilson L. Microtubules as a target for anticancer drugs. Nat Rev Cancer 2004; 4:253-65; PMID:15057285; DOI:10.1038/nrc1317.
49. Steigemann P, Wurzenberger C, Schmitz MH, Held M, Guizetti J, Maar S, et al. Aurora B-mediated abscission checkpoint protects against tetraploidization. Cell 2009; 136:473-84; PMID:19203582; DOI:10.1016/j.cell.2008.12.020.
50. Wittmann T, Hyman A, Desai A. The spindle: a dynamic assembly of microtubules and motors. Nat Cell Biol 2001; 3:28-34; PMID:11146647; DOI:10.1038/35050669.
51. Dumont S, Mitchison TJ. Force and length in the mitotic spindle. Curr Biol 2009; 19:749-61; PMID:19906577; DOI:10.1016/j.cub.2009.07.028.
52. Sharp DJ, McDonald KL, Brown HM, Matthies HJ, Walczak C, Vale RD, et al. The bipolar kinesin, KLP61F, cross-links microtubules within interpolar microtubule bundles of Drosophila embryonic mitotic spindles. J Cell Biol 1999; 144:125-38; PMID:9885249; DOI:10.1083/jcb.144.1.125.
53. Tanenbaum ME, Macurek L, Galjart N, Medema RH. Dynein, Lis1 and CLIP-170 counteract Eg5-dependent centrosome separation during bipolar spindle assembly. EMBO J 2008; 27:3235-45; PMID:19020519; DOI:10.1038/emboj.2008.242.
54. Mountain V, Simerly C, Howard L, Ando A, Schatten G, Compton DA. The kinesin-related protein, HSET, opposes the activity of Eg5 and cross-links microtubules in the mammalian mitotic spindle. J Cell Biol 1999; 147:351-66; PMID:10525540; DOI:10.1083/jcb.147.2.351.
55. Ferenz NP, Paul R, Fagerstrom C, Mogilner A, Wadsworth P. Dynein antagonizes eg5 by cross-linking and sliding antiparallel microtubules. Curr Biol 2009; 19:1833-8; PMID:19836236; DOI:10.1016/j.cub.2009.09.025.
56. Brunet S, Polanski Z, Verlhac MH, Kubiak JZ, Maro B. Bipolar meiotic spindle formation without chromatin. Curr Biol 1998; 8:1231-4; PMID:9811610; DOI:10.1016/S0960-9822(07)00516-7.
57. Schuh M, Ellenberg J. Self-organization of MTOCs replaces centrosome function during acentrosomal spindle assembly in live mouse oocytes. Cell 2007; 130:484-98; PMID:17693257; DOI:10.1016/j.cell.2007.06.025.
58. Khodjakov A, Cole RW, Oakley BR, Rieder CL. Centrosome-independent mitotic spindle formation in vertebrates. Curr Biol 2000; 10:59-67; PMID:10662665; DOI:10.1016/S0960-9822(99)00276-6.
59. Mahoney NM, Goshima G, Douglass AD, Vale RD. Making microtubules and mitotic spindles in cells without functional centrosomes. Curr Biol 2006; 16:564-9; PMID:16546079; DOI:10.1016/j.cub.2006.01.053.
60. Hornick JE, Mader CC, Tribble EK, Bagne CC, Vaughan KT, Shaw SL, Hinchcliffe EH. Amphiastral Mitotic Spindle Assembly in Vertebrate Cells Lacking Centrosomes. Curr Biol 2011.
61. Tulu US, Fagerstrom C, Ferenz NP, Wadsworth P. Molecular requirements for kinetochore-associated microtubule formation in mammalian cells. Curr Biol 2006; 16:536-41; PMID:16527751; DOI:10.1016/j.cub.2006.01.060.
62. Rello-Varona S, Vitale I, Kepp O, Senovilla L, Jemaa M, Metivier D, et al. Preferential killing of tetraploid tumor cells by targeting the mitotic kinesin Eg5. Cell Cycle 2009; 8:1030-5; PMID:19270519; DOI:10.4161/cc.8.7.7950.
63. Sakowicz R, Finer JT, Beraud C, Crompton A, Lewis E, Fritsch A, et al. Antitumor activity of a kinesin inhibitor. Cancer Res 2004; 64:3276-80; PMID:15126370; DOI:10.1158/0008-5472.CAN-03-3839.
64. Blagden SP, Molife LR, Seebaran A, Payne M, Reid AH, Protheroe AS, et al. A phase I trial of ispinesib, a kinesin spindle protein inhibitor, with docetaxel in patients with advanced solid tumours. Br J Cancer 2008; 98:894-9; PMID:18319713; DOI:10.1038/sj.bjc.6604264.
65. Zhang CC, Yang JM, White E, Murphy M, Levine A, Hait WN. The role of MAP4 expression in the sensitivity to paclitaxel and resistance to vinca alkaloids in p53 mutant cells. Oncogene 1998; 16:1617-24; PMID:9569030; DOI:10.1038/sj.onc.1201658.
66. Alli E, Bash-Babula J, Yang JM, Hait WN. Effect of stathmin on the sensitivity to antimicrotubule drugs in human breast cancer. Cancer Res 2002; 62:6864-9; PMID:12460900.
67. Balachandran R, Welsh MJ, Day BW. Altered levels and regulation of stathmin in paclitaxel-resistant ovarian cancer cells. Oncogene 2003; 22:8924-30; PMID:14654788; DOI:10.1038/sj.onc.1207060.
68. Martello LA, Verdier-Pinard P, Shen HJ, He L, Torres K, Orr GA, et al. Elevated levels of microtubule destabilizing factors in a Taxol-resistant/dependent A549 cell line with an alpha-tubulin mutation. Cancer Res 2003; 63:1207-13; PMID:12649178.
69. Kavallaris M. Microtubules and resistance to tubulin-binding agents. Nat Rev Cancer 2010; 10:194-204; PMID:20147901; DOI:10.1038/nrc2803.
70. Rowinsky EK, Donehower RC. Paclitaxel (taxol). N Engl J Med 1995; 332:1004-14; PMID:7885406; DOI:10.1056/NEJM199504133321507.
71. Blagosklonny MV, Darzynkiewicz Z. Cyclotherapy: protection of normal cells and unshielding of cancer cells. Cell Cycle 2002; 1:375-82; PMID:12548008; DOI:10.4161/cc.1.6.259.
72. Rao B, van Leeuwen IM, Higgins M, Campbel J, Thompson AM, Lane DP, et al. Evaluation of an Actinomycin D/VX-680 aurora kinase inhibitor combination in p53-based cyclotherapy. Oncotarget 2010; 1:639-50; PMID:21317459.